Sensors and Materials, Vol. 28, No. 5 (2016) 577–584
MYU Tokyo

S & M 1211

Effect of Nitrogen Implantation on the Performance of TOHOS Total Ionizing Dose Radiation Sensor Device

Wen-Ching Hsieh,* Hao-Tien Daniel Lee,[1] Fuh-Cheng Jong,[2] and Shich-Chuan Wu[3]

Department of Opto-Electronic System Engineering, Minghsin University of Science and Technology,
Xinxing Road 1, Xinfeng 30401, Taiwan
[1]Treasure Giant Technology Inc. 3F-1, 42, Lyushuei Road, Hsinchu 30068, Taiwan
[2]Electronic Engineering Department, Southern Taiwan University of Science and Technology,
1, Nan-Tai Street, Yungkang District, Tainan 710, Taiwan
[3]National Nano Device Laboratories, No. 26, Prosperity Road 1, Hsinchu Science Park, Hsinchu 30078, Taiwan

(Received September 1, 2015; accepted January 19, 2016)

Keywords: high k, sensor, TID, SONOS, SOHOS, MOS, radiation

The nitrogen-implanted titanium nitride–silicon oxide–hafnium oxide–silicon oxide–silicon (hereafter, N-TOHOS) device can be a candidate for total ionizing dose (TID) radiation sensor application. In this study, we mainly focus on N implantation for the improvement of the TID radiation-induced charging effect performance of the N-TOHOS device. The TID radiation-induced charging effect performance of the N-TOHOS device is improved by the implantation of nitrogen in the HfO_2 trapping layer. Experimental data show that the radiation-induced charge density of a typical N-TOHOS device is approximately 4–5 times that of a conventional metal–oxide–nitride–oxide–silicon (MONOS) device reported previously. The charge retention reliability after 5 mrad gamma irradiation of the N-TOHOS device with a high implantation dose and a low implantation energy can be improved. The N-TOHOS device described in this study has demonstrated its potential for nonvolatile TID radiation sensing application in the future.

1. Introduction

The total ionizing dose (TID) radiation effect is a major application concern for the operation of electronic devices in advanced X-ray lithography semiconductor manufacturing processes and outer space applications, as well as in other harsh environments such as accelerators, where high- and low-energy particles exist. After gamma irradiation, it is well known that the metal–silicon dioxide–silicon (MOS) structure shows a build-up of positive charges at the silicon–silicon dioxide (Si–SiO_2) interface and an interface state occurs in the structure.(1) The radiation-induced charging effects of a metal–nitride–silicon dioxide–silicon (MNOS) device with stacked insulation layers composed of silicon nitride and silicon dioxide have been reported.(2) TID radiation-induced charging effects in traditional silicon–silicon dioxide–nitride–silicon dioxide–silicon (SONOS) nonvolatile memory (NVM) devices have been studied.(3–5) Until now, little is known about the radiation response of SONOS-like devices with a high-k gate dielectric structure.(6,7) High-k gate dielectrics have been used for reducing the transistor gate leakage current in advanced nanoscale complementary metal-oxide-semiconductor (CMOS) devices.(8–10) Recently, the conventional

---

*Corresponding author: e-mail: wchsieh@must.edu.tw

SONOS flash memory has been replaced with the SOHOS memory device. However, the SOHOS device has very poor data retention characteristic.(8–10) The radiation-induced charging effect of a few hafnium-based MOS devices have been reported.(6,7) However, the data retention reliability of the hafnium-based SONOS-like device after gamma irradiation has not been well studied and it will be the main focus of this study.

To improve the charge retention reliability of the hafnium-based SONOS-like device after gamma irradiation, a nitrogen-implanted titanium nitride–silicon oxide–hafnium oxide–silicon oxide–silicon (hereafter, N-TOHOS) device is fabricated. The N-TOHOS device as illustrated in Fig. 1 is characterized by its delta V_T performance as a potential candidate TID radiation sensor in this study. The electrical performances of N-TOHOS devices with various implantation doses and energies after gamma irradiation, including charge storage density, gate leakage current, V_T stability, and retention time, are the main subjects of this study.

2. Experimental Details

N-TOHOS devices obtained under various nitrogen implantation conditions are listed in Table 1. The various devices denoted as N1-TONOS to N7-TOHOS were used throughout this study. N1-TONOS with a nitride-trapping layer and N2-TOHOS without nitrogen implantation were used for

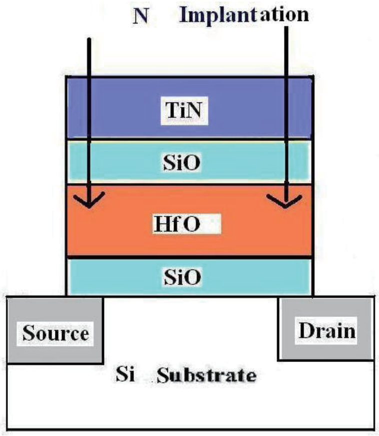

Fig. 1. (Color online) Cross-sectional view of N-TOHOS device.

Table 1
N-TOHOS devices prepared under various implantation conditions.

	N1-TONOS@	N2-TOHOS@	N3-TOHOS	N4-TOHOS	N5-TOHOS	N6-TOHOS	N7-TOHOS
Trapping layer	Si_3N_4	HfO_2	HfO_2	HfO_2	HfO_2	HfO_2	HfO_2
N implantation dose (cm^{-2})	No	No	1E+13 (LD)*	1E+14 (MD)*	1E+15 (HD)*	1E+15 (HD)*	1E+15 (HD)*
N implantation energy (keV)	No	No	5 (LE)#	5 (LE)#	5 (LE)#	7 (ME)#	9 (HE)#

@: N1-TONOS with nitride-trapping layer and N2-TOHOS without N implantation are used for comparison.
*LD, low dose; MD, medium dose; HD, high dose.
#LE, low energy; ME, medium energy; HE, high energy.

comparison. The N-channel TOHOS devices were fabricated at the Taiwan National Nano Device Laboratories (NDL, Hsinchu, Taiwan). Starting wafers were 6” silicon having a (100) orientation with boron-doped substrates and a resistivity of 15–25 Ω•cm. The tunneling silicon oxide (SiO_2) was formed by using an advanced clustered vertical furnace on the wafers and its thickness was 3–5 nm, which was measured using a spectroscopic ellipsometer. After the tunneling oxide formation, Si_3N_4 (100–200 Å) was deposited as charge-trapping layers by low-pressure chemical vapor deposition (LPCVD) for the N1-TONOS device. For the TOHOS devices, HfO_2 films were deposited as the charge-trapping layers using a metal organic chemical vapor deposition (MOCVD) system at 400–550 °C for an approximate thickness of 10–20 nm. The precursor Hf (tert-butoxy)$_2$ (mmp)$_2$ was used in the MOCVD system. The blocking oxide (100–200 Å thickness) was deposited by LPCVD using tetra ethyl oxysilane (TEOS) [$Si(OC_2H_5)_4$]. After blocking oxide deposition, the nitrogen implantation into HfO_2 was carried out at low energy (LE, 5 keV), medium energy (ME, 7 keV), and high energy (HE, 9 keV), with low dose (LD, 1E13 atoms/cm^2), medium dose (MD, 1E14 atoms/cm^2), and high dose (HD, 1E15 atoms/cm^2). The control gate with a 200–400 nm TiN metal gate was formed by DC sputtering for all samples. The resulting structure is illustrated in Fig. 1. After gate patterning, source and drain were formed by implantation with arsenic atoms, which were activated at 900 °C for 30 s. For comparison, all the devices listed in Table 1 have the same thicknesses of tunneling oxide, trapping oxide, and blocking oxide layer.

In this work, the V_T shifts due to gamma irradiation on the N-TOHOS devices prepared by various implantation methods were measured. The gamma irradiation was performed on the N-TOHOS devices with negative gate bias stress (NVS) ($V_G = -1$ V) using a ^{60}Co irradiator source at room temperature. The V_T changes of the N-TOHOS devices prepared by various implantation methods were examined after the gamma irradiation. V_T was measured at room temperature using a HP4156A parameter analyzer. The experimental results of gate leakage current under various gate voltages (I_G–V_G) were obtained using a computer-controlled HP4156 parameter analyzer. The experimental results of gate capacitance applied with various gate voltages (C_G–V_G) were obtained using a computer-controlled HP4284 parameter analyzer, and the C_G–V_G curves were obtained by sweeping V_G under zero source-and-drain bias condition at room temperature.

Figure 2 shows the charge generation and trapping states of the gate dielectric for the N-TOHOS device under NVS after gamma irradiation.

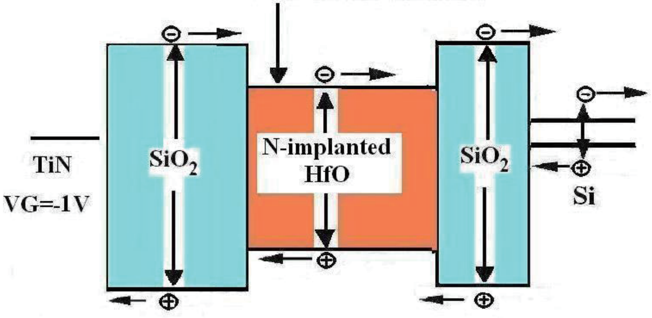

Fig. 2. (Color online) Charge generation and trapping states in N-TOHOS device under NVS after gamma irradation.

3. Results and Discussion

3.1 Radiation-induced charging effect of TOHOS after gamma irradiation

Figure 3 shows the I_D–V_G curve for a typical N5-TOHOS device with negative bias voltage (V_G = −1 V) and processed with gamma irradiation up to 5 mrad TID. A significant negative V_T shift of the N5-TOHOS device is observed in the figure, which is a result of the increase in positive charges in the trapping layer caused by ionization radiation. The negative V_T shift result agrees with those of previous studies.(5,6) The radiation-induced negative V_T shift in the irradiated N5-TOHOS device is induced by a combination of storage charge loss in the HfO_2 trapping layer and a build-up of positive charges from the asymmetric trapping of electrons and holes in the trapping layer.(5,6) As the N5-TOHOS device was irradiated by ionization radiation, the electron–hole pairs are generated throughout the gate insulation layer, and fractions of free electrons and holes escaped from the initial recombination process. The TID radiation-induced charging effect on the device is determined by the survival yield of electron–hole pairs, which is a portion of free holes and electrons that survived after the recombination process immediately following the excitation processes due to ionization radiation.

The |delta V_T| of the N5-TOHOS device increases as a function of gamma TID, as indicated in Fig. 4. It also shows a quasi-linear correlation of |delta V_T| vs gamma radiation TID below 100 krad in log scale, but |delta V_T| increases more sharply after gamma irradiation at levels up to 100 krad TID.(5,6) This result is in agreement with those of previous studies.(5,6)

The |delta V_T| and charge density comparisons after 5 mrad TID gamma irradiation for various N-TOHOS devices shown in Table 1 are illustrated in Figs. 5(a) and 5(b), respectively. The trapped charge density can be calculated by the Terman method.(7) The radiation-induced V_T shift of TOHOS without nitrogen implantation is more significant than that of TONOS, which results from more radiation-induced charges into the HfO_2 trapping layer than into the Si_3N_4 charging layer. Furthermore, the radiation-induced V_T shift increases with the implantation dose for the N-TOHOS device with the low implantation energy, as shown in Fig. 5(a). Note that the radiation-induced

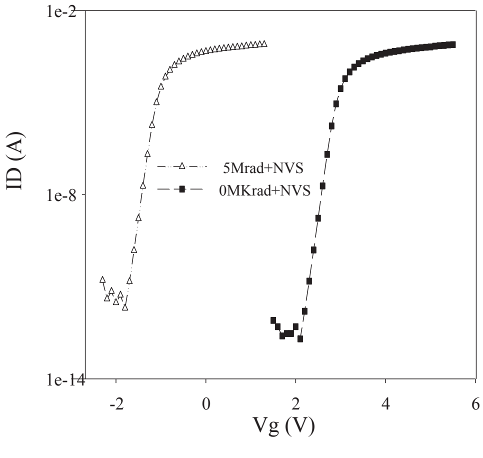

Fig. 3. I_D–V_G curve for N5-TOHOS device after 5 mrad TID gamma irradiation.

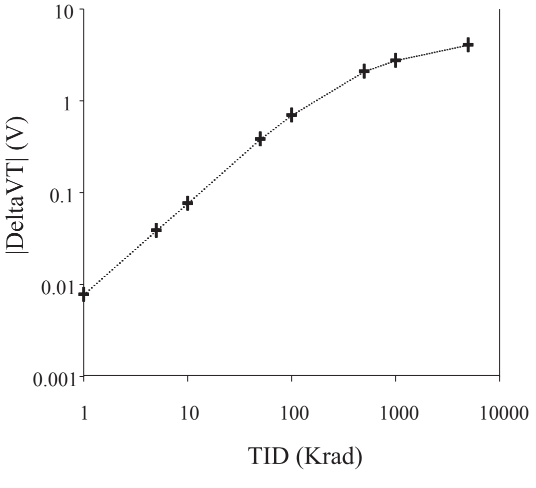

Fig. 4. |Delta V_T| increase as a function of gamma radiation TID for N5-TOHOS device.

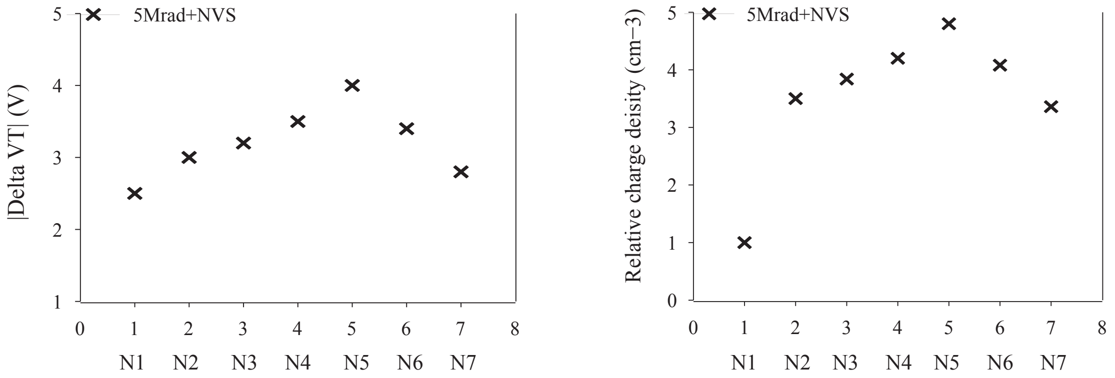

(a) (b)

Fig. 5. (a) |Delta V_T| comparison for N-TOHOS devices prepared by different implantation methods listed in Table 1 after 5 mad TID gamma irradiation. (b) Relative charge density comparison for various N-TOHOS devices after 5 mrad gamma irradiation.

charge density of the N5-TOHOS device with high-dose and low-energy implantation is 4.8 times larger than that of the TONOS device. Furthermore, The radiation-induced charging effect of the N5-TOHOS device is more significant than that of the metal-aluminum oxide–hafnium aluminum oxide–silicon oxide–silicon (MAHAOS) device reported previously.(6) The TID radiation-induced charging effect of the N-TOHOS device is improved by an increase in the amount of positive charges caused by gamma iradiation in the trapping layer, which is a result of the nitrogen atoms implanted in the HfO_2 trapping dielectric. However, the radiation-induced V_T shift decreases with the implantation energy for the N-TOHOS device with high implantation dose, which is a result of the high-energy-implantation damage of the HfO_2 trapping dielectric as shown in Fig. 5(a).

3.2 Gate leakage current measurement

Figure 6(a) and 6(b) show the gate leakage current for N-TOHOS devices prepared by various implantation methods after 10 krad and 5 mrad TID gamma irradiation, respectively. As shown in Fig. 6(a), the gate leakage current of TOHOS is extremely worse than that of TONOS after 10 krad and 5 mrad TID gamma irradiation, which is because more interface traps of HfO_2 lead to a larger gate current leakage after 10 krad and 5 mrad TID gamma irradiation.(7) The gamma irradiation could induce new crystallized phases and chemical structure change of HfO_2, which would lead to the generation of trapped charges and leakage current in the HfO_2 trapping layer.(7) However, by high-dose implantation of nitrogen into HfO_2, the gate leakage current performance is markedly improved after 10 krad and 5 mrad TID gamma irradiation. After high-dose implantation, nitrogen atoms might be trapped in the interface traps of $HfO_{2,}$ leading to the improvement of the gate current leakage. This result suggests that high-dose nitrogen implantation is very effective for improving the gate leakage current of the N-TOHOS device after 10 krad and 5 mrad TID gamma irradiation. However, the gate leakage current performance of the N-TOHOS device by high-energy implantation is worse than that of TONOS after 5 mrad TID gamma irradiation, which is a result of the high-energy-implantation damage of the blocking oxide and the charge leakage path after 5 mrad gamma irradiation.

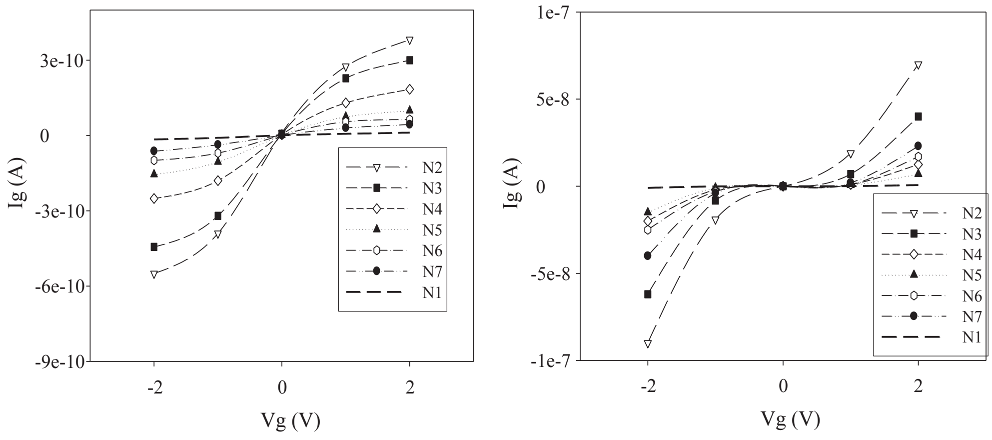

(a) (b)

Fig. 6. (a) $|I_G|$ ($V_G = -1$ V) comparison for various N-TOHOS devices after 10 krad gamma irradiation. (b) $|I_G|$ ($V_G = -1$ V) comparison for various N-TOHOS devices after 5 mrad gamma irradiation.

3.3 V_T stability vs retention time

In this section, the V_T stability and retention time of N5-TOHOS devices are discussed and these are the important electrical properties that need to be verified for their potential application in TID radiation sensors. Figure 7 shows the V_T stability vs retention time under NVS ($V_G = -1$ V) for the N5-TOHOS device after gamma irradiation. The upper curve is for V_T decay of N5-TOHOS after 10 krad TID gamma irradiation and the lower curve is for V_T decay of N5-TOHOS after 5 mrad TID gamma irradiation. Note that the V_T decay over time of the N5-TOHOS device after gamma irradiation is a result of charge tunneling from the nitrogen-implanted HfO_2 trapping layer. However, there is no noticeable decay trend of the V_T for the N5-TOHOS device after 5 mrad gamma irradiation. This trend can be attributed to a more effective charge recording ability inside the stack gate of the N5-TOHOS device after high-dose gamma irradiation.

Figures 8 and 9 show the V_T stability vs time under NVS ($V_G = -1$ V) for N-TOHOS devices prepared by various implantation methods after 10 krad and 1 mrad gamma irradiations, respectively. It is seen that the device with HfO_2 as the charge-storage layer shows the worse charge retention reliability characteristic than Si_3N_4. These results are consistent with the gate leakage results shown in Fig. 6(a) and mentioned earlier. Therefore, it seems that the device with HfO_2 is degraded in terms of charge storage capacity by providing stored charges with a leakage path. The worse charge storage capacity in the TOHOS device may be attributed to tunneling leakage current induced by interface trap states.(8) However, by applying high-dose and high-energy implantation of nitrogen into HfO_2, the charge retention performance is markedly improved after 10 krad and 1 mrad gamma irradiations. The charge retention reliability performance of the N-TOHOS device is improved owing to the deep traps induced by nitrogen implantation in the HfO_2 trapping layer after 10 krad and 1 mrad gamma irradiations.(8,9)

Figure 10 shows the V_T stability versus time under NVS ($V_G = -1$ V) of N-TOHOS devices prepared by various implantation methods after 5 mrad gamma irradiation. However, for high-

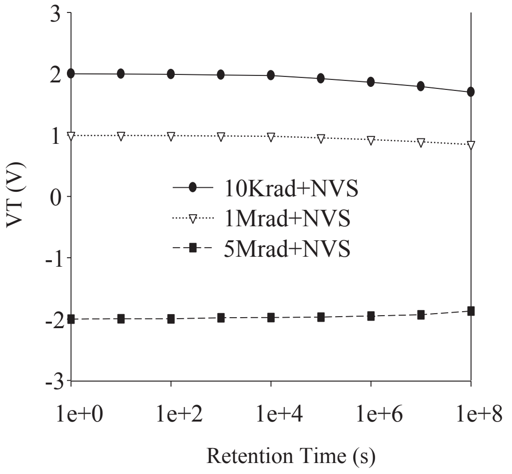

Fig. 7. V_T stability under $V_G = -1$ V for N5-TOHOS devices after gamma irradiation.

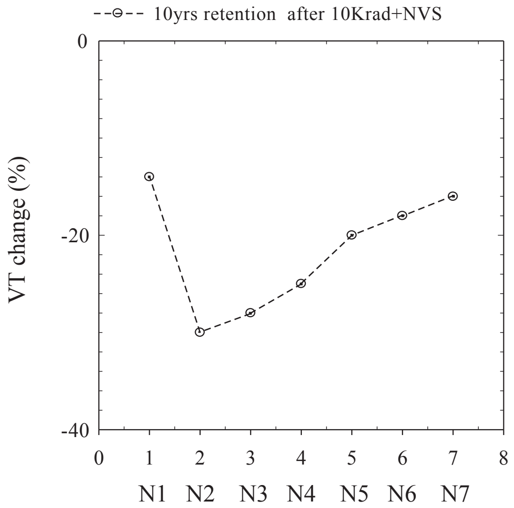

Fig. 8. V_T change with 10-y retention time under $V_G = -1$ V for various N-TOHOS devices after 10 krad gamma irradiation.

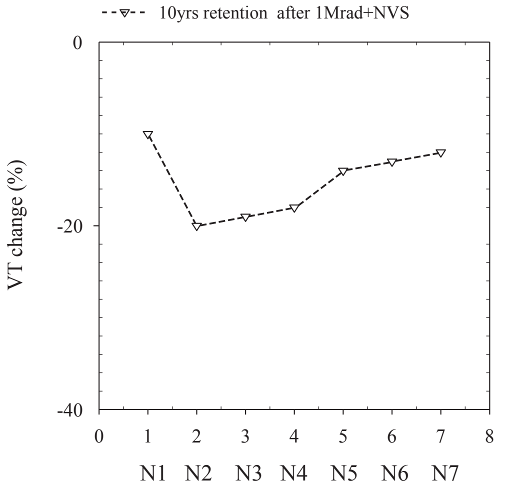

Fig. 9. V_T change with 10-y retention time under $V_G = -1$ V for various N-TOHOS devices after 1 mrad gamma irradiation.

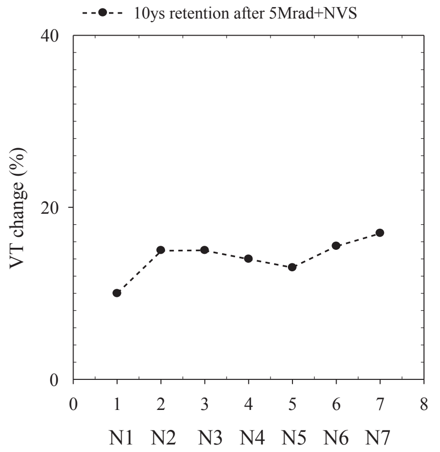

Fig. 10. V_T change with 10-y retention time under $V_G = -1$ V for various N-TOHOS devices after 5 mrad gamma irradiation.

energy nitrogen-implanted N5-TOHOS devices, the charge retention reliability characteristics after 5 mrad gamma irradiation show the opposite trend with those after 10 krad gamma irradiation. The charge retention reliability characteristic for N7-TOHOS device after 5 mrad gamma irradiation is considerably worse than those for other devices prepared by other implantation methods after 5 mrad gamma irradiation, which is a result of the high-energy-implantation damage of the blocking oxide and the charge leakage path through the blocking oxide after 5 mrad gamma irradiation.

4. Conclusions

The radiation-induced V_T shifts increase with the implantation dose for N-TOHOS devices with low-energy implantation. Furthermore, by applying high-dose and high-energy implantation of nitrogen into HfO_2, the charge retention reliability performance is markedly improved after 10 krad gamma irradiation. However, the charge retention reliability characteristic for N7-TOHOS device after 5 mrad gamma irradiation is considerably worse than those for other devices, which is a result of the high-energy-implantation damage of the blocking oxide and the charge leakage path through the blocking oxide after high-dose gamma irradiation. The results show that N-TOHOS with a high implantation dose and a low implantation energy can be a potential candidate nonvolatile TID radiation sensor in the future.

Acknowledgements

The authors would like to thank the NDL, National Tsing Hua University (NTHU), and National Chiao Tung University (NCTU) for providing the instruments for wafer fabrication and testing. This study was funded in part by the National Science Council (NSC).

References

1 K. Watanabe, M. Kato, T. Okabe, and M. Nagata: IEEE Trans. Nucl. Sci. **33** (1986) 1216.
2 Y. Takahashi, K. Ohnishi, T. Fujimaki, and M. Yoshikawa: IEEE Trans. Nucl. Sci. **46** (1999) 1578.
3 A. Gasperin, G. Ghidini, A. Cester, and A. Paccagnella: IEEE Trans. Nucl. Sci. **54** (2007) 1898.
4 B. Draper, R. Dockerty, M. Shaneyfelt, S. Habermehl, and J. Murray: IEEE Trans. Nucl. Sci. **55** (2008) 3202.
5 F. Y. Qiao, X. Yu, and L.Y. Pan: Proc. 19th Int. Symp. Phys. Fail. Anal. Integr. Circuits (IPFA) (IEEE, Singapore, 2012) pp. 1–4.
6 W. C. Hsieh, H. T. Lee, and F. C. Jong: Sensors **14** (2014) 14553.
7 Y. Cheng, M. Ding, X. Wu, X. Liu, and K. Wu: 2013 Int. Conf. Solid Dielectrics. (IEEE, Italy, 2013) pp. 764–767.
8 J. G. Park, J. S. Oh, S. D. Yang, K. S. Jeong, Y. M. Kim, H. J. Yun, H. D. Lee, and G. W. Lee: Proc. Nanotechnol. Mater. Devices Conf. (IEEE, California, 2010) pp. 364–367.
9 L. J. Liu, K. S. Chang-Liao, T. Y. Wu, T. K. Wang, W. F. Tsai, and C. F. Ai: Microelectron. Eng. **86** (2009) 1852.
10 B. Y. Tsai,. B. Y. Tsui, P. Li, and C. C. Yen: IEEE EDL. **32** (2011) 1594.